On-off intermittencies in gas discharge plasma

D. L. Feng,* C. X. Yu, J. L. Xie, and W. X. Ding†
Department of Modern Physics, University of Science and Technology of China, Hefei, Anhui 230026, People's Republic of China
(Received 14 January 1998)

In this paper we report two on-off intermittency phenomena observed in a gas discharge plasma system. The laminar phase distribution of the intermittencies is studied in various situations. The Poincaré bifurcation and another type of bifurcation, namely, ''period-period'' bifurcation, are identified as the underlying system dynamics, respectively. Based on these bifurcations, numerical models are constructed, which basically explain most of the experimental observations. A theoretical discussion is also presented. [S1063-651X(98)08908-9]

PACS number(s): 52.35.Ra, 05.45.+b

I. INTRODUCTION

Intermittency, quasiperiodic chaos, and period-doubling chaos are three well-known routes to chaos. Because intermittency is generally defined as random disruption of a quiescent or laminar state by a turbulent or bursting state, it is the most common chaotic phenomenon in physical systems and numerical models. From Pomeau and Manneville's early type-I, -II, and -III intermittencies [1] to Price and Mullin's type-*X* intermittency [2], from crisis-induced intermittency [3] to recent type-*V* intermittency [4], it has become manifest as a very active area of chaos research in the past decades. Recently, another dynamic intermittent phenomenon, on-off intermittency, has been introduced by Platt *et al.* [5]. Since then, many theoretical [6,7] and numerical [8–11] studies have been conducted on this issue. However, only a few pieces of experimental evidence in electrical circuits have been reported so far [12,13]. In this article we report the experimental observation of two on-off intermittency phenomena in a gas discharge plasma system. One of them is observed near a Poincaré bifurcation point and the other results from a different type of bifurcation. The laminar length distribution, one of the most important properties for intermittency, is studied in detail and found to have an exponential scaling law for the former, but to be very complicated for the latter. The return map and other properties are also studied. Numerical studies are also carried out and the results agree with the experiments very well.

The mechanism for on-off intermittency is a dynamic time-dependent force on a bifurcation parameter through a bifurcation point, which differs from the other types of intermittency that occur for fixed parameter values beyond the bifurcation point. Therefore, a nonlinear system with the parameter driven randomly or chaotically through a bifurcation point will move among several branches of bifurcation and will exhibit a chaotic mixing of those states, thus generating on-off intermittency. In this sense, on-off intermittency differs from other types of intermittency also in that it depends not on a specific type of bifurcation but on any bifurcation that can be steered. This also necessitates that on-off intermittency would widely exist in nonlinear systems with an abundance of bifurcations. Since we have found very rich chaotic and bifurcation phenomena in a gas discharge plasma [14–16], it certainly should be an ideal physical system in which to search for and study on-off intermittency.

II. EXPERIMENTAL SETUP

The experiment was performed in a large multidipole steady-state plasma device as described in Ref. [14]. The device consists of an electron-emitting cathode and current-collecting anode. The argon plasma is produced by a dc discharge between the anode and cathode. The typical plasma parameters measured by a Langmuir probe are electron density $n_e = 10^7 - 10^8$ cm^{-3}, electron temperature $T_e = 1-3$ eV, and ion temperature $T_i \ll T_e$. The discharge is determined by the argon pressure (P_{Ar}), filaments current (I_f), discharge voltage (V_D), and separation between the anode and the cathode (d). All those parameters are relevant to the bifurcations observed in the plasma. However, for fast and easy real time control of the bifurcation parameter, only the discharge voltage V_D is suitable. As shown in Fig. 1, the steering signal generated by the computer is transferred to the controllable voltage source by a 12-bit digital/analog converter to produce a perturbation voltage V_S, which together with a fixed dc voltage V_{dc} and the voltage across filament V_f forms the total discharge voltage $V_D = V_{\mathrm{dc}} + V_S + V_f$. V_f is more than 5 V, depending on I_f. In most of the

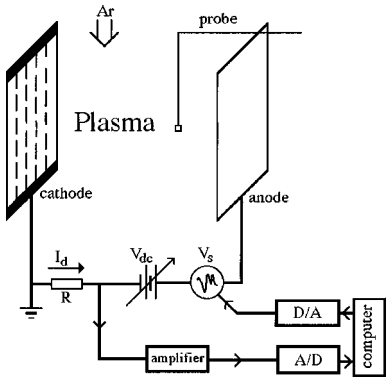

FIG. 1. Diagram of the on-off intermittency experimental arrangement.

*Present address: Department of Physics, Stanford University, Stanford, CA 94305.

†Present address: Oak Ridge National Laboratory, Oak Ridge, TN 38831-6122.

experiments, where V_S is not so large, V_D is kept well above the argon ionization potential (15.7 V), so that the plasma discharge is maintained throughout the experiment. On the other hand, when the perturbation signal is very large, the discharge might be extinguished during the experiment. However, a larger steering signal also generates on-off intermittency with shorter laminar lengths. Therefore, we can usually accumulate about 10^4 laminar lengths before the system collapses.

For simplicity and to get somewhat quantifiable results, white noise and Gaussian noise are selected as the forms of V_S in most of the experiments and the amplitude is defined as a_w for white noise with the identity distribution in the interval $[-0.5a_w, 0.5a_w]$ and zero otherwise, or as σ for Gaussian noise with the distribution function $(1/\sqrt{2\pi\sigma})e^{-x^2/2\sigma^2}$. Other steering wave forms such as the chaotic signals generated by the well-known Lorentz or Rossler attractor are also used in some of the experiments, which will be discussed in Sec. V. In order to get the distribution of the laminar length l of these on-off intermittencies, the discharge current signal I_d is acquired by an analog/digital (12-bit) converter. Both analog/digital and digital/analog converters are designed to be able to work in a continuous mode, so that we can measure an ultralong laminar state, thus getting more reliable statistical results of the laminar length. The laminar lengths are collected after each 128 kbytes of data has been taken, which determines the upper limit of the laminar length we can get to be about 13 s. This time scale is much larger than the time scale of the intermittencies addressed here (1 ms–1000 ms). The lower limit of the laminar length l_0 is defined to be 1.5 times the period of the plasma oscillations (0.5–1.5 ms, depending on the experimental parameters), so we will not take a long laminar oscillating phase as many short laminar phases. Finally, the laminar length distribution $P(l)$ is obtained by constructing a histogram of the recorded l's and $P(l)$ is the number of cases falling in the small region around l, which is not normalized throughout this paper.

III. POINCARÉ BIFURCATION BASED ON-OFF INTERMITTENCY

The Poincaré bifurcation is a common nonlinear process through which a system changes from a fixed point to a limit cycle state. For example, consider the well-known Van der Pol equation [17]

$$\ddot{x}+\mu(x^2-1)\dot{x}+x=0 \tag{1}$$

in $(x,\dot{x})$ phase space. When $\mu<0$, (0,0) is a stable focus, $\mu=0$ a center, and $\mu>0$ an unstable point surrounded by a stable limit cycle with finite radius. So the system will suddenly jump from a static state (fixed point O) to a periodic state (limit cycle) when the control parameter μ goes up through the bifurcation point $\mu=0$. In our plasma system, the same bifurcation is also observed when we keep $I_f=22.4$ A, $P_{\mathrm{Ar}}=9\times10^{-4}$ Torr, and $d=90$ mm but decrease V_{dc} gradually from 20 V. At first, the plasma system is in a dc discharge state, but when $V_{\mathrm{dc}}=14.1$ V, a periodic self-oscillation state suddenly appears [18] [as shown in the inset of Fig. 2(a)]. This oscillation continues until V_{dc} reaches 13 V, where further bifurcation happens. In the experiment, we set $V_{\mathrm{dc}}=15$ V, so the system is placed in the dc discharge side of the bifurcation. Then we choose either white or Gaussian noise generated by two pseudorandom number algorithms as the randomly steering signal V_S. The amplitude of this perturbation signal, a_w or σ, is gradually increased. As indicated in Fig. 2(a), when it exceeds some critical value, an oscillation signal suddenly appears in the discharge current signal. When a_w or σ becomes larger, oscillations appear more frequently, which is shown in Fig. 2(b). We define the dc discharge state as the ''off'' state and the oscillation as the bursting ''on'' state. The length of the off state is the so-called laminar length.

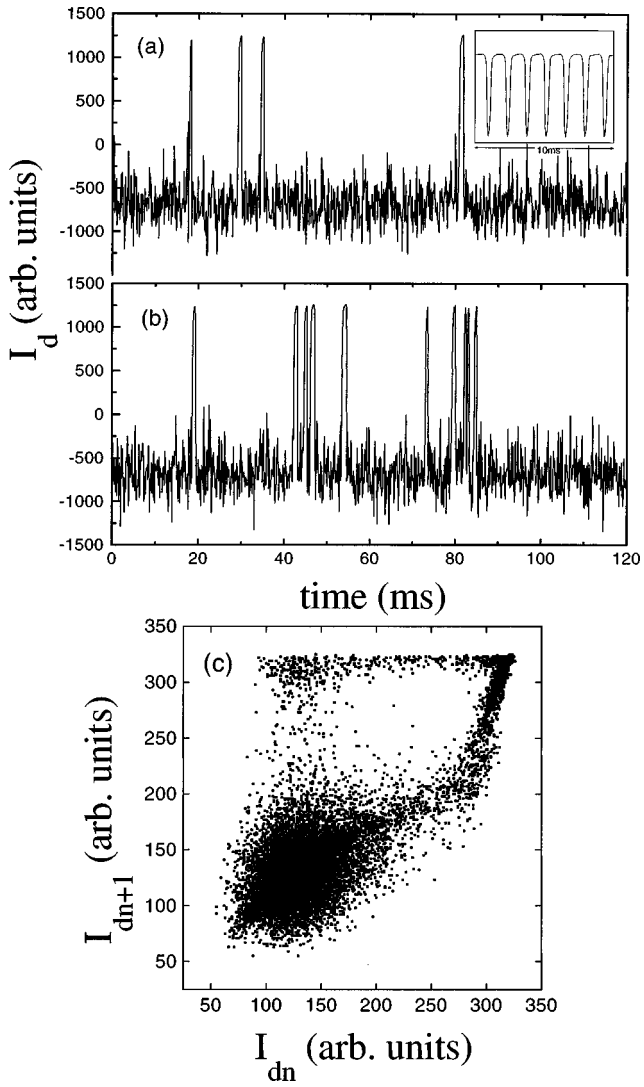

FIG. 2. Typical on-off intermittency signal of the plasma discharge current I_d under (a) small steering force and (b) larger steering force, and (c) the corresponding return map, where the black spot and the limit cycle are expanded by the noise signal. The inset of (a) is the unperturbed I_d oscillation signal.

Figure 2(c) shows the return map constructed from the data that has been partially plotted in Fig. 2(b). The black spot on the left bottom is the fixed point and the circle is the limit cycle; these correspond to the dc discharge state and the oscillating state, respectively. The hopping of the system between these two states is the on-off intermittency resulting

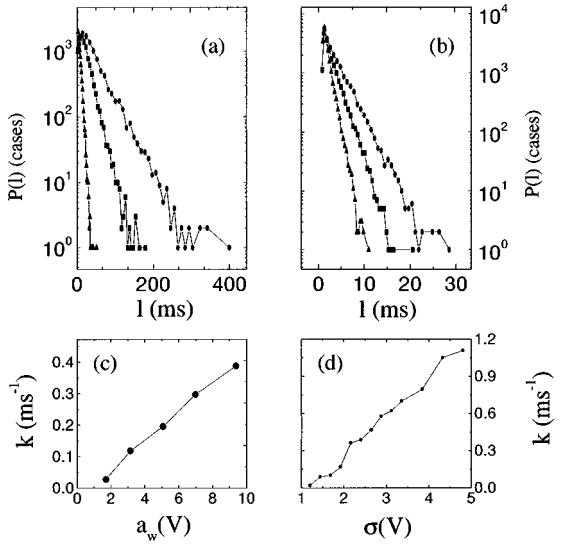

FIG. 3. Semilogarithmic plot of the experimental laminar length distribution $P(l)$ in the (a) white noise driven cases at $a_w = 1.704$, 3.624, and 5.064 V from right to left and (b) Gaussian noise driven cases at $\sigma = 2.16$, 2.88, and 4.32 V from right to left. It is clear that $P(l) \sim e^{-kl}$. The corresponding relations of k in $P(l)$ and the amplitude of the steering force are shown in (c) and (d).

from the Poincaré bifurcation.

The distribution of the laminar length is plotted in Figs. 3(a) and 3(b) for white and Gaussian noise steering, respectively. With the increase of the perturbation strength, the distribution curve becomes steeper, indicating the decrease of the average laminar length $\langle l \rangle$. The distributions for both the white and Gaussian noise steering case exhibit an almost perfect exponential law $P(l) \propto e^{-kl}$, where k is constant. This result is different from the power-law distribution with an exponent $-3/2$ observed by other groups, which will be discussed later. For such an exponential law of laminar length distribution, a simple mathematical derivation will give that the mean laminar length $\langle l \rangle = l_0 + 1/k$. Therefore, k basically reflects the response of the system to the driving force. Figures 3(c) and 3(d) give the relation of k and the amplitudes of white noise and Gaussian noise, respectively. It can be found that k increases almost linearly with the increase of the noise amplitudes. Moreover, it is observed that Gaussian noise leads much more effectively to the on-off intermittency than white noise. This implies that to get the same k value of the distribution $P(l)$ a much larger amplitude for white noise steering is required than for Guassian noise. This is because white noise is a bounded noise process, for example, $[-1,1]$, while Gaussian noise is a unbounded one. Even with a very small amplitude, the ''high-energy tail'' in Gaussian noise makes it possible for the steered control parameter to reach and go through the critical bifurcation point.

To the author's knowledge, no specific investigation has been done on the on-off intermittency based on the Poincaré bifurcation. In order to gain insight into the features of the on-off intermittency observed in our experiment further, a numerical study of the on-off intermittency was carried out with the Van der Pol oscillator system. As stated before, $\mu = 0$ is the Poincaré bifurcation point in the Van der Pol system. $\mu_{dc} = -0.1$ is selected as the unperturbed offset control parameter, so the system initially stays in the fixed point

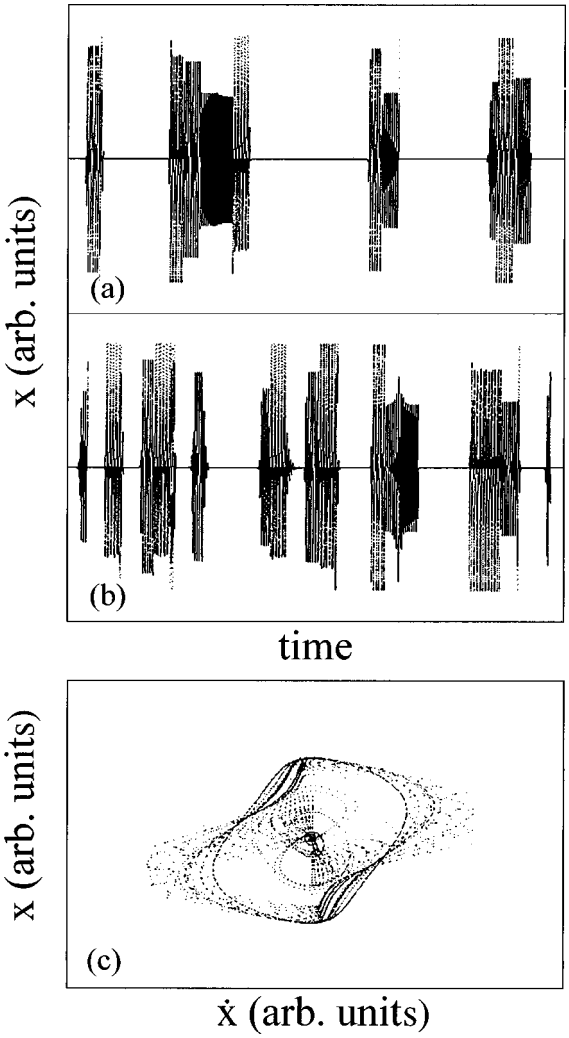

FIG. 4. On-off intermittency phenomena in the Van der Pol oscillator when the steering force is (a) small and (b) larger. 3×10^5 data points or 3×10^3 unit time of data are used. (c) is the corresponding return map.

state. Then the steering noise μ_S is added to μ_{dc}. Here the shortest time scale of the steering noise is chosen as $(2-3)T_0$, where T_0 is the period of the oscillation, to simulate the fast response of the plasma to the change in the control parameter due to the steering noise. Simulation results are shown in Figs. 4(a) and 4(b). The steering of μ makes the system hop between the fixed point and the limit cycle oscillation state. Figure 4(c) shows the return map constructed from the data in Fig. 4(a). Similar to Fig. 2(c), this return map also consists of a fixed point and a limit cycle around it. Defining the fixed point as the off state, the laminar length distributions are shown in Figs. 5(a) and 5(b) for white and Gaussian noise driving cases. It is obvious that $P(l)$ of this numerical model for the on-off intermittency also obeys the same exponential law as the experimental ones. In Figs. 5(c) and 5(d) the relations between the steering noise amplitude and k are shown. When the steering noise is not so big, k changes with it linearly, just as we have found in the experiments [see Figs. 3(c) and 3(d)]. However, when steering increases, k tends to saturate to some constant, which we failed to verify in the experiment because a new bifurcation happened when it went too far and sometimes the whole system collapsed.

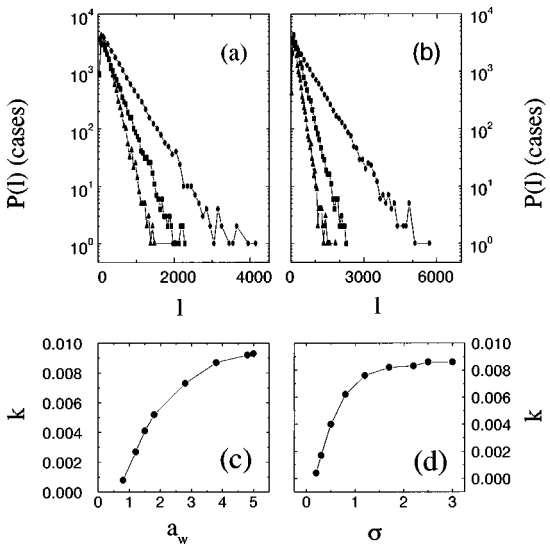

FIG. 5. Numerical laminar length distribution for (a) white and (b) Gaussian noise steering at $\mu_{dc}=-0.1$. From the right curve (ovals) to the left one (triangles), (a) $a_w=1.2$, 1.5, and 1.8 and (b) $\sigma=0.3$, 0.5, and 0.8. The corresponding numerical relations of k in $P(l)$ and the steering signal amplitude are shown in for (c) the white noise steering case and (d) the Gaussian noise steering case. All quantities are regarded as dimensionless in the model equation.

So far, the numerical results agree with the corresponding experimental ones very well both phenomenologically and qualitatively. This suggests that the experimental founding of on-off intermittency based on the Poincaré bifurcation in the discharge plasma system is not just a system-dependent specific one, but one that has a general meaning.

IV. PERIOD-PERIOD BIFURCATION AND RELATED ON-OFF INTERMITTENCY

In the preceding section we described how the system evolves from a dc discharge state to an oscillation state (for simplicity we call this the Y oscillation) and the on-off intermittency that is based on this Poincaré bifurcation. As the discharge voltage $V_{\rm dc}$ is lowered further to about 13.5 V, a new oscillation signal, whose period is only about 1/3 of that of the Y oscillation (it is called the X oscillation for the same reason), will appear together with the Y oscillation. The lower the $V_{\rm dc}$, the more frequently the X oscillation appears until it replaces the Y oscillation after $V_{\rm dc}$ is less than 13 V. This phenomenon has been identified as the system becomes unstable through a tangent bifurcation, with two coexistent attractor-repellor evolving to repellor-attractor, respectively. A type-I intermittency based on this continuous bifurcation has been studied in Ref. [16].

After the system has finished the tangent bifurcation, it will stay in the X-oscillation state for a certain range of $V_{\rm dc}$. However, after the discharge voltage $V_{\rm dc}$ is decreased to a certain value V_{DZ}, which is about 11.5 V, the X oscillation suddenly disappears and another type of oscillation (called the Z oscillation) with half the amplitude of the X oscillation appears instead. The system will stay in the Z-oscillation state for another range of $V_{\rm dc}$. Then, if $V_{\rm dc}$ is increased, the system will return to the X-oscillation state at some value $V_{DX}\approx 12$ V and V_{DX} is larger than V_{DZ}. This process is

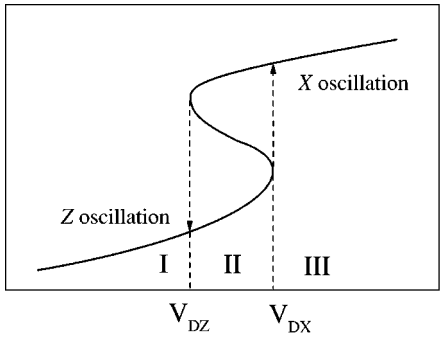

FIG. 6. Schematic illustration of the period-period bifurcation. The X oscillation and Z oscillation can jump to each other at V_{DZ} and V_{DX}, respectively. Three experimental V_{dc} are selected in regions I, II, and III.

illustrated in Fig. 6. To the author's knowledge, this kind of sudden change between two periodic states with dynamic bistability has not been studied in depth. Here we call it a period-period bifurcation.

In order to study the on-off intermittency based on the period-period bifurcation, three $V_{\rm dc}$ values, 11.4, 11.85, and 12.15 V, are selected in the regions $V_{\rm dc}<V_{DZ}$, $V_{DZ}<V_{\rm dc}<V_{DX}$, and $V_{DX}<V_{\rm dc}$, which are called the control parameter regions I, II, and III, respectively, in Fig. 6. Then the steering noise signal V_S is added. The typical on-off intermittency signals of the discharge current I_d produced by the driving voltage $V_{D,i}=V_{{\rm dc},i}+V_{S,i}+V_f$, where $V_{{\rm dc},i}$ are the dc offset voltages in regions $i=$I, II, and III and $V_{S,i}$ is their steering noise beyond the thresholds, are shown in Fig. 7. The signals look very similar under these three conditions, where X and Z oscillations appear randomly in the time series. The dotted lines in the figures indicate the steering noise, which is switched on and off to study the relation of the coexistent states and the on-off intermittency. It can be seen that when the steering noise is switched off while the system is in the on-off intermittency state, the system may stay in either the X- or the Z-oscillation state. However, when $V_{\rm dc}$ is in region I or III, the system staying in the X- or the Z-oscillation state is unstable and will eventually return

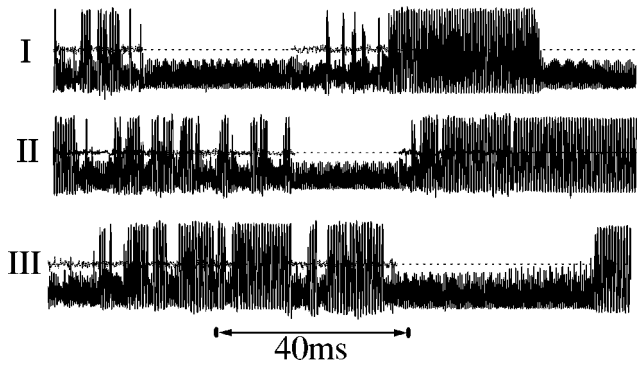

FIG. 7. From top to bottom are the three I_d signals corresponding to experimental condition in regions I, II, and III. The dotted line is the steering noise signal, which is switched on and off in the experiment. When it is on, I_d is in the on-off intermittency state; otherwise I_d will be in the X or Z state. However, X (Z) is unstable in region I (III), so it will go to the stable Z (X) state at some point. The arrowed line indicates the time scale of 40 ms.

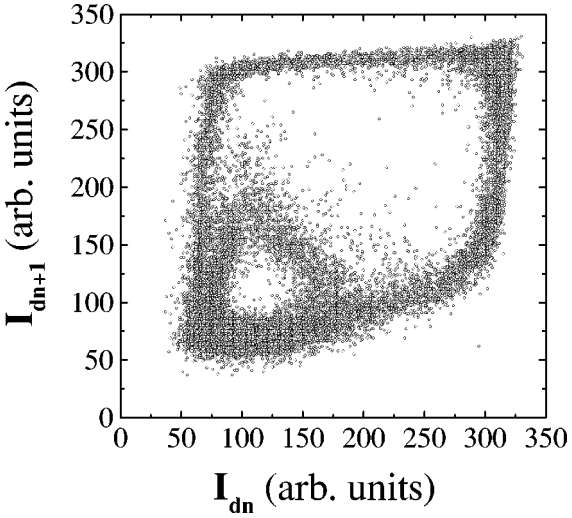

FIG. 8. Return map constructed from typical on-off intermittency data. The two loops indicate the two limit cycles; the larger one represents the X oscillation and the smaller one represents the Z oscillation. These two limit cycles overlap each other in some region. The system jumps between these two limit cycles in the on-off intermittency state.

to the Z- or the X-oscillation state. This clearly shows the relation between the X and Z attractors (or repellors) and their stability changing with V_{dc}. The return map of this on-off intermittency is plotted in Fig. 8, which clearly shows the coexistence of the two corresponding limit cycles and the transition between them.

If the on state is assigned to the X oscillation and the off state to the Z oscillation, the laminar length distribution function $P(l)$ can be determined. As shown in Fig. 9(a), in the cases of $V_{\mathrm{dc}}>V_{DX}$ and $V_{\mathrm{dc}}<V_{DZ}$, that is, when there is only one attractor in the system, $P(l)$ still has an exponential law distribution. However, it is more complicated for the case of $V_{DZ}<V_{\mathrm{dc}}<V_{DX}$. Figures 9(b) and 9(c) show the distributions for the case of V_{dc} set in region II with white and Gaussian noise steering, respectively. There are two characteristics of these plots distinguishing them from Fig. 9(a). The first is the appearance of humplike structures in $P(l)$; these structures incrementally disappear as V_S increases. The second is that $P(l)$ has a bisection form at large V_S: for large l, $P(l)\sim e^{-kl}$; for small l, $P(l)\sim l^{-\delta}$. This distribution is similar to the theoretical result of Heagy *et al.* [7] for the tangent bifurcation based on-off intermittency, whose $P(l)\sim l^{-\delta}e^{-kl}$ with $\delta=3/2$. The distributions for large V_S are shown in a log-log plot in Fig. 9(d), whose upper left portion shows a power law distribution with $\delta=1.5\pm0.1$ and 1.0 ± 0.1 for the Gaussian and white noise steering cases, respectively.

Since we could not find the corresponding mathematical model for the period-period bifurcation, we built a classical mechanical model to simulate this phenomenon. Consider a particle moving in a central potential field with the shape plotted in Fig. 10(a). The particle's total energy E is selected as the control parameter. When $E<E_{cZ}$, the particle will be constrained in the inner potential well; when $E>E_{cX}$, it can move in the whole potential; when $E_{cX}>E>E_{cZ}$, the particle can move in the outer or inner potential well depending on its initial position. Taking the movement in the inner potential well (smaller radius) as Z-type movement and in the outer potential well (larger radius) as X-type movement, this model may be analogous to the bistable period-period bifurcation observed in the experiment.

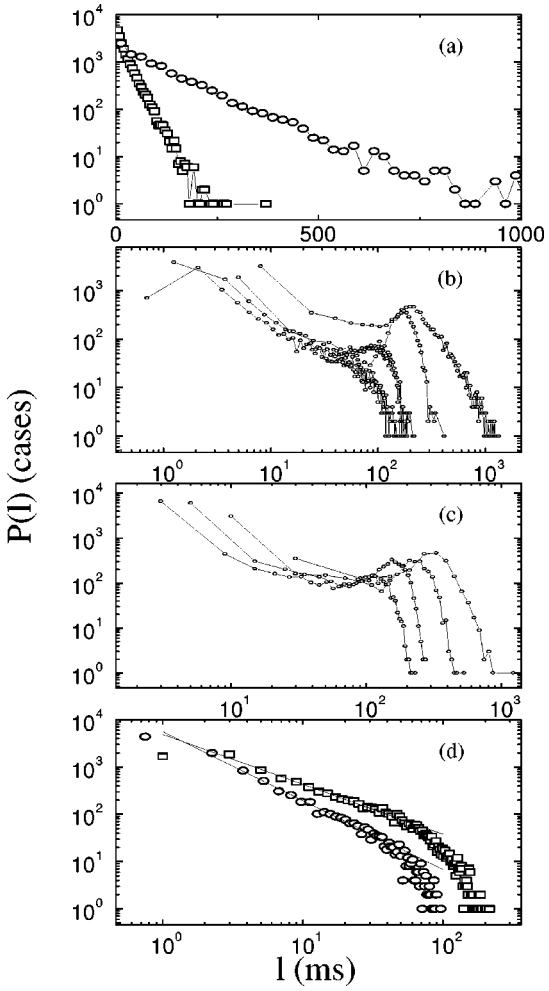

FIG. 9. $P(l)$'s of the period-period bifurcation based on-off intermittency when (a) $V_{dc}<V_{DZ}$ (open rectangle, $\sigma=0.22$ V) and $V_{dc}>V_{DX}$ (open oval, $\sigma=0.163$ V); (b) $V_{dc}\in[V_{DZ},V_{DX}]$ and the steering white noise amplitude $a_w=0.552$, 0.624, 0.864, and 0.912 V from the right curve to the left one; (c) $V_{dc}\in[V_{DZ},V_{DX}]$ and the steering Gaussian noise amplitude $\sigma=0.0768$, 0.096, 0.12, and 0.144 V from the right curve to the left one; and (d) $V_{dc}\in[V_{DZ},V_{DX}]$ and the steering white noise amplitude $a_w=0.96$ V (open rectangles) and the steering Gaussian noise amplitude $\sigma=0.216$ V (open ovals). In the linear-logarithmic plot (a) the distributions are exponential in form, while in the log-log plot (b) and (c) the distributions are suppressed from some ''hump'' structure (right curves) to the $l^{-\delta}e^{-kl}$ form (left curves) with the increment of the steering signal amplitude until they finally reach the shapes shown in (d), where the fitting lines have a slope of -1 ± 0.04 for the white noise case (open rectangles) and -1.5 ± 0.05 for the Gaussian noise case (open ovals).

In the polar coordinate system, we can easily get the equation for this system:

$$\ddot{r}-\frac{2[E-V(r)]-\dot{r}^2}{r}=-\nabla V(r). \tag{2}$$

Setting $x=r$ and $y=\dot{x}$, we get a two-dimensional system

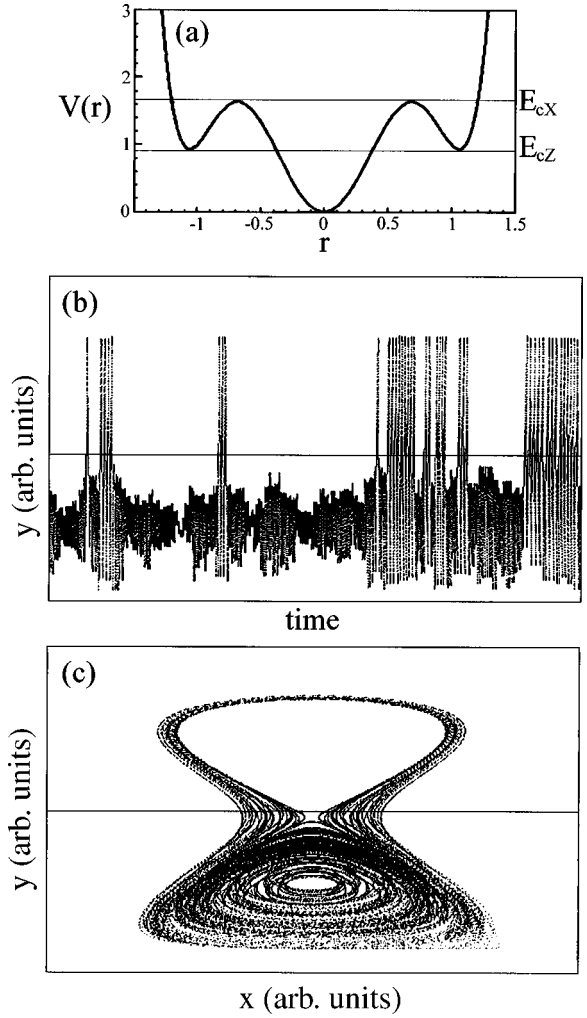

FIG. 10. Numerical model for the period-period bifurcation and the corresponding on-off intermittency. (a) The double-well potential $V(r)$ and the transition points E_{cZ} and E_{cX}. (b) The typical on-off intermittency signal. Because 10^5 data points are plotted, one cannot distinguish them in some regions. (c) The corresponding return map. The outer and bigger circles represent the X-type motion and those inside are from the Z-type motion.

$$\dot{x}=y, \quad \dot{y}=-\frac{dV(x)}{x}+\frac{2[E-V(x)]-y^2}{x}, \tag{3}$$

where $V(x)=a_6x^6+a_4x^4+a_2x^2$ and a_6, a_4, a_2 are constants.

Similarly to the experiment, we define X-type movement as the on state and Z-type movement as the off state. Perturbation noise is added to the total energy E to get the on-off intermittency. To simulate the situation of $V_{\rm dc}\notin[V_{DZ},V_{DX}]$ in the experiment, $E_{\rm dc}$ is set to 0.8. If the noise amplitude is large enough, on-off intermittency can be observed as shown in Fig. 10(b), which is very similar to the experimental one for time series. The corresponding return map and the off state distribution $P(l)$ are shown in Figs. 10(c) and 11(a), respectively. The $P(l)$ found here also obeys the e^{-kl} law, which agrees with the experimental result well. Similarly, in order to simulate the $V_{\rm dc}\in[V_{DZ},V_{DX}]$ situation, $E_{\rm dc}$ is selected as 1.6. The time series and return map under this condition are similar to that of the $V_{\rm dc}\notin[V_{DZ},V_{DX}]$ case. However, as seen in Fig. 11(b), the corresponding $P(l)$ in this case is found to be a bisection distribution: for small l, $P(l)\sim l^{-\delta}$; for large l, $P(l)\sim e^{-kl}$. It is exactly what we have found in the experiment. Furthermore, for the power law portion of the distribution, the exponent is found to be -1.56 ± 0.08 and -1.0 ± 0.1 for the Gaussian and white noise steering cases, respectively. These results also agree with the experimental observations.

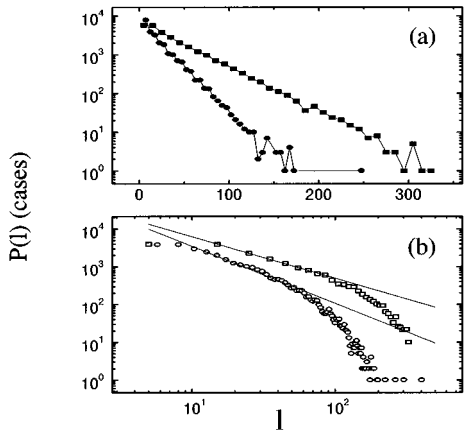

FIG. 11. Numerical laminar length distribution $P(l)$ for the classical mechanical model at (a) $E_{dc}=0.8$, $\sigma=0.5$ (solid rectangles) and $\sigma=0.6$ (solid ovals), where $P(l)\sim e^{-kl}$ and with larger steering signal the curve becomes steeper, and (b) $E_{dc}=1.6$, where $P(l)\sim e^{-kl}l^{-\delta}$. The open oval curve corresponds to the case of Gaussian noise steering with $\sigma=0.18$ and the open rectangle curve corresponds to the case of white noise steering with $a_w=0.4$. The two fitting lines have slopes of -1.5 and -1.0, respectively.

When the steering noise amplitude is increased further, the $P(l)$ becomes an exponential law distribution. However, unfortunately, this cannot be verified in the experiment because the system will break under large steering noise. Also the ''hump'' in the experimental $P(l)$ has not been observed in the numerical simulation.

The on-off intermittency described in this section is different from other known on-off intermittencies. Its $P(l)$ has a very complex structure. This may result from the dynamic details of the two interacting attractor and repellor and their basins.

V. DISCUSSION AND SUMMARY

In the previous experiment, numerical simulation, and also other related works, one can see that the laminar length distribution $P(l)$ of on-off intermittency has various forms, which include e^{-kl}, $l^{-\delta}$, $e^{-kl}l^{-\delta}$, and even some complex structures such as the hump found here in the period-period bifurcation case. So a natural question arises whether there are some general mechanisms behind all these forms of $P(l)$.

Suppose there is a nonlinear system exhibiting on-off intermittency and its behavior can be monitored by a one-dimensional system variable y (just like the I_d used in our plasma system). From the mathematical point of view, this system variable y is a random variety and the on-off intermittency due to the noise source driving system is a random process $y(t)$. For simplicity, suppose that the system is discrete. Then $y(t)$ can be rewritten as $y_i(i\in Z)$. Defining y_c as

a small threshold below which y_i is considered to be in the off state, a state with laminar length of n is defined as $\{y_i \leqslant y_c, i=1,2,\ldots,n, y_{n+1}>y_c\}$. Therefore, the probability for an off state with such a laminar length to happen is

$$P_n = \mathrm{Prob}\left[\bigcap_{j=1}^{n} y_j \leqslant y_c \cap y_{n+1} > y_c\right]. \tag{4}$$

Generally, a system's current state is not only related to the current system control parameter, but it is also related to its previous states. If y_j is related to its previous M step's values $y_{j-1}, y_{j-2}, \ldots, y_{j-M}$, then the random process can be regarded as an Mth-order Markov process. Formula (4) can now be rewritten as

$$\begin{aligned} P_n = {} & \mathrm{Prob}[y_1 \leqslant y_c | y_0, y_{-1}, \ldots, y_{1-M}] \\ & \times \mathrm{Prob}[y_2 \leqslant y_c | y_1, y_0, \ldots, y_{2-M}] \\ & \times \cdots \times \mathrm{Prob}[y_n \leqslant y_c | y_{n-1}, y_{n-2}, \ldots, y_{n-M}] \\ & \times \mathrm{Prob}[y_{n+1} > y_c | y_n, y_{n-1}, \cdots, y_{n-M+1}]. \end{aligned} \tag{5}$$

The simplest case is $M=0$ and we have

$$\begin{aligned} P_n^0 = {} & \mathrm{Prob}[y_1 \leqslant y_c]\mathrm{Prob}[y_2 \leqslant y_c] \\ & \times \cdots \mathrm{Prob}[y_n \leqslant y_c]\mathrm{Prob}[y_{n+1} > y_c]. \end{aligned} \tag{6}$$

In the case of the white or Gaussian noise steering, $\mathrm{Prob}[y < y_c] = \lambda$, so

$$P_n^0 = \lambda^n \Big/ \sum_{j=0}^{\infty} \lambda^j = \frac{1-\lambda}{\lambda}\lambda^n \equiv c e^{-kn}, \tag{7}$$

where $c \equiv (1-\lambda)/\lambda$ and $k \equiv -\ln \lambda$.

Formula (5) is a general expression of a high-order Markov process. So to get the laminar length distribution, one needs not only the probability of a state at the current system control parameters but also the transition probabilities. The latter is directly related to the dynamic details of the system. When the system reacts to the control parameter perturbation very slowly, there will be a long transition state. As a result, the position of the system in the phase space, the details of the steering signal (which is not necessarily a noise signal), the properties of the underlying bifurcation, and other factors will affect the final state. The corresponding $P(l)$ is certainly a complex one. One may not expect a common distribution form of $P(l)$ in the on-off intermittency case as $l^{-1/2}$ for type-I intermittency and l^{-2} for type-II intermittency. Actually, this is also due to the fact that on-off intermittency is not just based on one particular type of bifurcation. Heagy *et al.* [7] proved that for a simple class of systems parametrically driven one-dimensional maps $y_{n+1} = p_n y_n + O(y_n^2)$, with p_n a random variable $P(l) \sim l^{-3/2} e^{-kl}$. This is an example of the general formula (5). Our numerical study found that in the system of the form $y_{n+1} = p_n y_n + O(y_n^{1.2})$, $P(l) \sim l^{-1} e^{-kl}$ [as shown in Fig. 12(a)]. This means that the finding of a $-3/2$ power law distribution in the small l region is not a universal scaling for the on-off intermittency ''family.''

On the contrary, if the system reacts very quickly to the change in control parameter, M tends to be 0. As a result, the system behavior and the control parameter are almost one to one and we will have a common $P(l)$ with the exponential form as shown in Eq. (7). Because the discharge plasma system we studied here has a very small time scale that is far smaller than that of the steering noise, we found an exponential form of $P(l)$ in the Poincaré bifurcation based on-off intermittency and the period-period bifurcation based on-off intermittency in parameter regions I and III. Furthermore, we can verify this point in the Van der Pol system. Figure 12(b) is the numerical result with Gaussian noise steering, whose time scale now is chosen as $0.1T_0$ here. Since the noise's time scale is small enough now, we get $P(l) \sim l^{-3/2} e^{-kl}$.

The situation is much more complex in the period-period bifurcation based on-off intermittency observed in parameter region II. In this condition both limit cycles are stable attractors and to make things ''worse,'' these two attractors overlap each other as shown in the return map (see Fig. 8). Therefore, the system is far more sensitive to the perturbation and

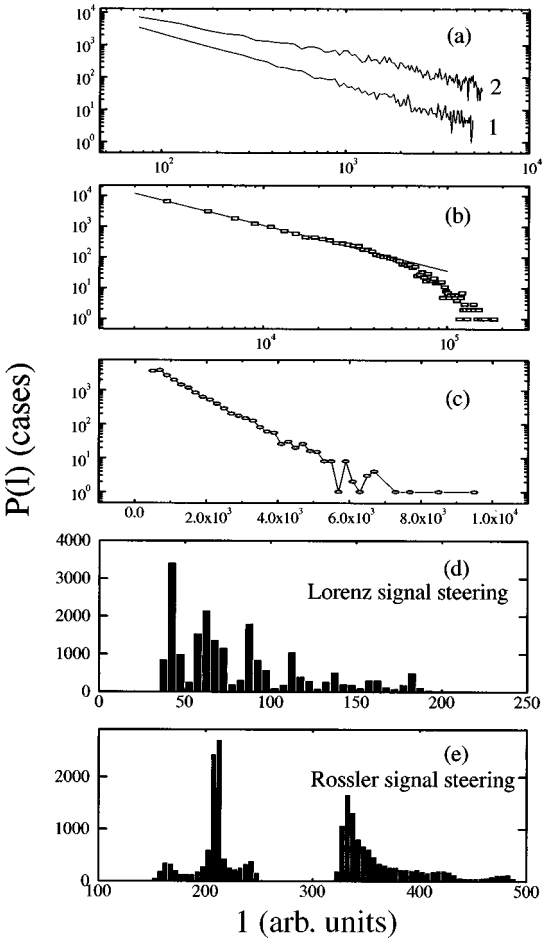

FIG. 12. Numerical simulation results of the laminar length distribution $P(l)$ for (a) the $y_{n+1} = p y_n + 0(y_n^{\alpha})$ type of on-off intermittency, where curve 1 corresponds to $\alpha = 2$, which has a slope of -1.5, while curve 2 corresponds to $\alpha = 1.2$, which has a slope of -1.0, (b) the Poincarè bifurcation based on-off intermittency when the steering Gaussian noise has a smaller time scale, where the straight line inside has a slope of -1.5, and (c) the period-period bifurcation based on-off intermittency in the parameter region II when the steering noise has a much larger time scale, where $P(l)$ has an exponential form, and the experimental $P(l)$ results for the Poincarè bifurcation based on-off intermittency with (d) a Lorentz chaotic signal and (e) Rossler chaotic signal steering.

its current position in the phase space. The response speed of the system is not the only critical factor in this case. That is why we saw the complex distribution functions in Fig. 9. In the numerical experiment, only if we make the noise time scale much larger or make its amplitude very large can we get an e^{-kl} type of $P(l)$ that is plotted in Fig. 12(c).

The simple driving forces, white and Gaussian noise used here, contribute to the simple forms of $P(l)$. On the other hand, in the Poincaré based on-off intermittency, experiments with driving chaotic signals from the Lorentz and Rossler systems give very complex $P(l)$ distributions, whose histogram plots are shown in Figs. 12(d) and 12(e).

To summarize, we have observed the Poincaré bifurcation based on-off intermittency and period-period bifurcation based on-off intermittency in a discharge plasma system driven by some noise signals. Numerical studies are also conducted, whose results generally agree with the experiment. It is also confirmed that these two types of on-off intermittencies are not only limited in plasma system. The laminar length distribution function $P(l)$ is studied in detail and found to be related to the system response time scale, property of steering signal, and system dynamic details. Therefore, some special form of $P(l)$ is not a characteristic to identify on-off intermittency, although $P(l)$ is still one of the most important characteristics of it.

ACKNOWLEDGMENTS

D.L. thanks Professor W. G. Ma and Dr. P. J. White for their help with the preparation of this article. This work is supported by the National Basic Research Project ''Nonlinear Science,'' Doctoral Training Foundation of National Education Commission, and Huo Yindong Education Foundation.

[1] Y. Pomeau and P. Manneville, Commun. Math. Phys. **74**, 189 (1980).
[2] T. J. Price and T. Mullin, Physica D **48**, 29 (1991).
[3] C. Grebogi *et al.*, Phys. Rev. Lett. **48**, 1507 (1987).
[4] M. Bauer, S. Habip, D. R. He, and W. Martienssen, Phys. Rev. Lett. **68**, 1625 (1992).
[5] N. Platt, E. A. Speigel, and C. Tresser, Phys. Rev. Lett. **70**, 279 (1993).
[6] N. Platt, S. M. Hammel, and J. F. Heagy, Phys. Rev. Lett. **72**, 3498 (1994).
[7] J. F. Heagy, N. Platt, and S. M. Hammel, Phys. Rev. E **49**, 1140 (1994).
[8] H. L. Yang and E. J. Ding, Phys. Rev. E **50**, R3295 (1994).
[9] F. Xie, G. Hu, and Zhilin Qu, Phys. Rev. E **52**, R1265 (1995).
[10] J. Redondo, E. Roldan, and G. J. de Valcarcel, Phys. Lett. A **210**, 301 (1996).
[11] Y. C. Lai and C. Grebogi, Phys. Rev. E **52**, 3313 (1995).
[12] P. W. Hammer, N. Platt, S. M. Hammel, J. F. Heagy, and B. D. Lee, Phys. Rev. Lett. **73**, 1095 (1994).
[13] Young Hun Yu, Keumcheol Kwak, and Tong Kun Lim, Phys. Lett. A **198**, 34 (1995).
[14] Jiang Yong, Wang Haida, and Yu Changxuan, Chin. Phys. Lett. **4**, 489 (1988); Jiang Yong, Doctoral dissertation, University of Science & Technology of China, 1988 (unpublished).
[15] Ding Weixing, Huang Wei, Wang Xiaodong, and C. X. Yu, Phys. Rev. Lett. **70**, 170 (1993).
[16] D. L. Feng, J. Zheng, W. Huang, C. X. Yu, and W. X. Ding, Phys. Rev. E **54**, 2839 (1996).
[17] Lu Qi-Shao, *Bifurcation and Singularity* (Shanghai Science-Technology Education Press, Shanghai, 1995).
[18] W. X. Ding, T. Klinger, and A. Piel, Phys. Lett. A **222**, 409 (1996).